

A new indirect multi-step-ahead prediction model for a long-term hydrologic prediction

Chun-tian Cheng^{1,*} Jing-Xin Xie^{2,3} Kwok-Wing Chau⁴ Mehdi Layeghifard⁵

¹Department of Civil Engineering, Dalian University of Technology, Dalian, 116024, P.R. China

²College of Mechanical and Electronic Engineering, Hebei Agricultural University, Baoding 071001, P.R. China

³Département d' Informatique, Université du Québec à Montréal (UQÀM), Montréal H2X 3Y7, QC, Canada

⁴Department of Civil and Structural Engineering, Hong Kong Polytechnic University, Hung Hom, Kowloon, Hong Kong

⁵Département des Sciences Biologiques, Université du Québec à Montréal (UQÀM), Montréal H2X 3Y7, QC, Canada

Abstract: A dependable long-term hydrologic prediction is essential to planning, designing and management activities of water resources. A three-stage indirect multi-step-ahead prediction model, which combines dynamic spline interpolation into multilayer adaptive time-delay neural network (ATNN), is proposed in this study for the long term hydrologic prediction. In the first two stages, a group of spline interpolation and dynamic extraction units are utilized to amplify the effect of observations in order to decrease the errors accumulation and propagation caused by the previous prediction. In the last step, variable time delays and weights are dynamically regulated by ATNN and the output of ATNN can be obtained as a multi-step-ahead prediction. We use two examples to illustrate the effectiveness of the proposed model. One example is the sunspots time series that is a well-known nonlinear and non-Gaussian benchmark time series and is often used to evaluate the effectiveness of nonlinear models. Another example is a case study of a long-term hydrologic prediction which uses the monthly discharges data from the Manwan Hydropower Plant in Yunnan Province of China. Application results show that the proposed method is feasible and effective.

Keywords: time-delay neural network, adaptive time-delay neural network, indirect multi-step-ahead prediction, spline interpolation

1. Introduction

A dependable long-term hydrologic prediction is essential to planning, designing and management activities of water resources (Lin et al., 2006; Sivakumar et al., 2001; Mimikou and Rao, 1983). During the past few decades, a great deal of research has been devoted to the formulation and development of approaches and models to improve the quality of hydrological prediction, including mechanistic models and black-box models (Karunasinghe and Liang, 2006; Chau, 2006; Cheng et al., 2006; Lin et al., 2006; Wu and Chau, 2006; Chau et al., 2005; Liang et al., 2005; Cheng et al., 2004; Arora, 2002; Islam and Sivakumar, 2002; Ismailov and Fedorov, 2001; Sivakumar et al., 2001; Irvine and Eberhart, 1992). Hydrological processes vary both spatially and temporally with a high nonlinearity in spatial and temporal scales (Parasuraman and Elshorbagy, 2007). The mechanistic models used to model such processes would require a large amount of high-quality data associated with astronomical, meteorological, natural geographical characteristics as well as human activity (Arora, 2002; Maier and Dandy, 1999; Milly, 1994), while the burden of data constrains the application of mechanistic models. In the other hand, the black-box models, that at first were only designed to identify the connection between inputs and outputs, are widely applied to forecast the long-term streamflow because of their requirement of little data and their simple formulation. The earlier methods include time series techniques and multiple linear regression methods (Smith, 1991; Irvine and Eberhardt, 1992). As an alternative to the aforementioned mathematical models, ANNs, which map the input to

* Chun-Tian Cheng, Corresponding author. Professor, Department of Civil Engineering, Dalian University of Technology, Dalian, 116024, P.R. China. Tel: +86-411-84708768. Fax: +86-411-84674141 Email: ctcheng@dlut.edu.cn

47 output without the need to identify the physics a priori, have been widely applied to
48 hydrology field (ASCE Task Committee, 2000; Luk et al., 2000; Maier and Dandy, 1999;
49 Atiya et al., 1999). Some applications of ANNs in long-term hydrologic prediction can be
50 found in the literature (Parasuraman and Elshorbagy, 2007; Karunasinghe and Liong, 2006;
51 Kisi, 2004).

52

53 For many engineering applications, a series of forecasts with a long ahead time are required.
54 In recent decades, multi-step-ahead (MS) techniques (Williams and Zipser, 1995), which can
55 predict time series values of many time-steps into the future and are classical model
56 predictive algorithms, have been developed to achieve this goal. MS prediction can be
57 divided into direct and indirect categories which have their own advantages and
58 disadvantages. Direct MS prediction models employ all the observations as inputs, while the
59 indirect models use the recursive method of single-step (SS) predictor. Theoretically, the
60 former models provide more precise results in comparison to the later models. However, the
61 direct prediction demands the model hold more flexible ability for each step prediction.
62 Furthermore, it is not easy to develop a direct prediction model. This is why we focus on
63 developing a new indirect multi-step-ahead prediction model in this research.

64

65 The difficulty of developing MS predictors is because of the lack of measurements in the
66 prediction horizon that necessitates the recursive use of SS predictors for reaching the
67 end-point in the horizon. Even small SS prediction errors at the beginning of the horizon
68 accumulate and propagate, often resulting in poor prediction accuracy. The situation is even
69 worse for complex systems which are characterized by poorly understandable, noisy, and
70 often nonlinear dynamics (Parlos et al., 2000). Recently, the recurrent neural network was
71 proven to be able to improve MS-based prediction and found to attain promising performance
72 (Bone and Crucianu, 2002; Khotanzad et al., 1994). However, training of a recurrent neural
73 network is usually very time consuming and a single recurrent neural network might lack in
74 robustness (Ahmad and Zhang, 2002). Relatively, feedforward network is easy to implement
75 with a low complexity regarding time and space. Time-delay neural network (TDNN) and
76 adaptive time-delay neural network (ATNN) were proven to be able to improve the
77 efficiency of the MS prediction. TDNN, introduced by Waibel (Waibel et al., 1989) who
78 employed time delays on connections in feedforward networks, has been successfully applied
79 in many areas (Haffner and Waibel, 1992; Luk et al., 2000; Ng and Cook, 1998; Shi et al.,
80 2003; Tan and Cauwenberghe, 1999; Yamashita, 1997). An adaptive version of TDNN, called
81 ATNN, which was originally proposed by Day (Day and Davenport, 1999) adapts its
82 time-delay values and its weights to better accommodate to changing temporal patterns, and
83 also to provide more flexibility for optimization tasks. It has also been successfully utilized in
84 nonlinear system identification (Lin et al., 1995; Yazdizadeh and Khorasani, 2002;
85 Yazdizadeh et al., 2000). In the case of single stage MS prediction, the main idea behind
86 both TDNN and ATNN is time-delay technology which utilizes current and delayed (or past)
87 observations of the measured system inputs and outputs as inputs to the network (Parlos et al.,
88 2000). As a result of time-delay technology, error iteration can deteriorate prediction
89 accuracy very quickly with increased steps ahead. Naturally, to improve the MS prediction, it
90 is required to reduce the use of iterative forecast values and add the observed values. Luckily,
91 the interpolation for discrete sequences (Mery et al., 1998; Schafer and Rabiner, 1973;
92 Tarczynski et al., 1994; Unser, 1999), which is usually employed in signal processing, can be
93 used for this purpose. In our study, the spline interpolation is employed to expend the
94 measurement data space of the model inputs and to increase the effect from observations.
95 Moreover, ATNN can provide more flexibility for optimization tasks.

96

97 In this paper, a three-stage MS prediction model, which combines dynamic spline
 98 interpolation into multilayer ATNN (SATNN), is proposed. In the first stage, the discrete time
 99 series, which has a uniform interval considered as original sampling frequency, is enlarged
 100 into many derivative sequences with various sampling frequencies by spline interpolating
 101 approximation. In the next stage, the input data set of ATNN variables for each prediction
 102 step is dynamically constructed through the integration of the derivative sequences
 103 mentioned above. In the last stage, parameters of the two previous stages, variable time
 104 delays, and weights are dynamically regulated by ATNN and therefore the output of ATNN
 105 can be obtained as a multi-step-ahead prediction. Using interpolation algorithm, some
 106 dynamic virtual data are inserted into the original sequences at a point far from the current
 107 spot. Therefore, the impact of the insertion of the prediction errors of the previous steps into
 108 the next step will be decreased and the reliability of this indirect multi-step-ahead prediction
 109 model will be improved. To illustrate the advantages of the proposed model, two examples
 110 are used. One example is the sunspots time series that is a well-known benchmark nonlinear
 111 and non-Gaussian time series and is often used to evaluate the effectiveness of nonlinear
 112 models(Zhang, 2003). Another is a case study of a long-term hydrologic prediction which
 113 uses the monthly discharges data from the Manwan Hydropower Plant in Yunnan Province,
 114 China.

115 2. Brief review on MS prediction, spline interpolation and ATNN

116 2.1 MS prediction

117 The recursive relation between inputs and outputs in MS prediction is defined as

$$118 \hat{x}_{t+p} = F(\hat{x}_{t+p-1}, \hat{x}_{t+p-2}, \dots, x_t, \dots, x_{t+p-s}) \quad (1)$$

119 Where p is the MS prediction horizon, s is the input dimension, and \hat{x}_{t+p} is an estimate of
 120 the output at time-step $t+p$. From equation (1), \hat{x}_{t+p} not only depends on the observation
 121 values but also on the previous predictions. The prediction accuracy deteriorated very quickly
 122 with increased p . An approach to improve the prediction accuracy is to enlarge the
 123 observation sample.

124 2.2 Cubic spline interpolation for discrete sequences(Kahaner et al., 1988)

125 The problem for cubic spline interpolation is described as we know a table of points $[x_i, y_i]$
 126 for $i=0,1,\dots,n$. And the function $y = f(x)$ estimates the value of a function for arbitrary x in a
 127 set of points $a = x_0 < x_1 < x_2 < \dots < x_n = b$. The function $s(x)$ is called a cubic spline on $[a, b]$ if

- 128 1) $s(x)$ is defined on $[a, b]$;
- 129 2) $s(x)$ and its first and second derivative, i.e., $s'(x)$ and $s''(x)$, are all continuous
 130 functions on $[a, b]$;
- 131 3) There are points (knots of the spline $s(x)$) such that $a = x_0 < x_1 < x_2 < \dots < x_n = b$ and
 132 $s(x)$ is a polynomial of degree ≤ 3 on each subinterval $[x_{i-1}, x_i]$

133 The fundamental idea behind cubic spline interpolation is used to draw smooth curves
 134 through a number of points. A third degree polynomial $s_i(x)$ is determined by

$$135 S_i(x) = M_{i-1} \frac{(x_i - x)^3}{6h_i} + M_i \frac{(x - x_{i-1})^3}{6h_i} \quad (2)$$

$$+ \left(y_{i-1} - \frac{M_{i-1} h_i^2}{6} \right) \frac{x_i - x}{h_i} + \left(y_i - \frac{M_i h_i^2}{6} \right) \frac{x - x_{i-1}}{h_i} \quad (i=1, 2, \dots, n)$$

136 Where $M_i = S_i''(x_i)$, $h_i = x_i - x_{i-1}$. Using the four conditions of cubic splines (Pollock, 1999),
 137 we can draw the following equation.

$$138 \quad h_i M_{i-1} + 2(h_i + h_{i+1})M_i + h_{i+1}M_{i+1} = 6 \left(\frac{y_{i+1} - y_i}{h_{i+1}} - \frac{y_i - y_{i-1}}{h_i} \right) \quad (3)$$

139 $i = 1, 2, \dots, n-1$

139 These equations can be much simplified if divided by $h_i + h_{i+1}$. Let $\lambda_i = \frac{h_{i+1}}{(h_i + h_{i+1})}$, $\mu_i = 1 - \lambda_i$
 140 and $d_i = 6 \left[\frac{y_{i+1} - y_i}{h_{i+1}} - \frac{y_i - y_{i-1}}{h_i} \right] / (h_i + h_{i+1})$. The equation (3) is translated into

$$141 \quad \mu_i M_{i-1} + 2M_i + \lambda_i M_{i+1} = d_i \quad (i = 1, 2, \dots, n-1) \quad (4)$$

142 Note that this system has n-2 rows and n columns, and is therefore under-determined. In
 143 order to generate a unique cubic spline, two other conditions must be imposed upon the
 144 system. There are various methods of the stipulation to be imposed upon the system. Natural
 145 spline is one of methods. Let the second derivative be equal to zero at the endpoints, i.e.,
 146 $M_1 = M_n = 0$. This results in the spline extending as a line outside the endpoints. Other
 147 second derivatives are determined accordingly. Correspondingly, $s_i(x)$ can be obtained.

148
 149 Using spline interpolation methods, we can increase sampling points between observations.
 150 Therefore, the estimated quality of \hat{x}_{t+p} will be improved once these interpolated values are
 151 pushed into current and delayed (or past) observations of the measured system input and
 152 output in equation 1.

153 2.3 Dynamic ATNN structure

154 ATNN adapts its time-delay values as well as its weights during training to better
 155 accommodate to changing temporal patterns and to provide more flexibility for optimization
 156 tasks (Day and Davenport 1999; Lin, et al., 1995; Yazdizadeh, 2002). A dynamic neuron
 157 structure is proposed by Lin et. al. (1995) and shown in Figure 1. The input-output mapping is
 158 then governed by

$$159 \quad y(t) = \sigma \left(\sum_{i=1}^M \omega_i x_i(t - \tau_i) \right) \quad (5)$$

160 where ω_i 's are the neuron weights, τ_i 's are the delays, and $\sigma(\cdot)$ is a nonlinear activation
 161 function. It has been shown that, even by taking the above simplified assumption, the resulting
 162 input-output map is still capable of representing the nonlinear system (Waibel et al., 1989).
 163 For the continuous time series, the time point t is rational sampling point, while in our study it
 164 is observation time. It should be noted that the output of the neuron at time t , which depends
 165 on the previous values of the outputs, results in a dynamic behavior. This dynamics will be
 166 modified subsequently for representing the nonlinear system.

167 *INSERT Figure 1 NEAR HERE*

168 3. SATNN model architecture and algorithm

169 The basic idea behind the design of the model is to use higher temporal resolution (i.e., a higher
 170 sampling rate and higher frequencies) for the long-term history and to use lower temporal

171 resolution for the short-term history (human brain uses a similar approach when combining
 172 the “detailed” certain-memory with the “general” uncertain-memory to predict future events).
 173 By this means, we get more essential information on the “detailed” and “general” history of
 174 the time series while we use a relatively small number of inputs in the forecasting system.
 175 With interpolation algorithm, some dynamic virtual data which can be called the “detailed”
 176 are inserted into the original sequences at the point far from the current spot. So the impact of
 177 previous prediction errors that would be iterated into the model for the next step prediction is
 178 decreased. Therefore, the reliability of this indirect multi-step-ahead prediction model will be
 179 improved when we make multi-step ahead prediction.

180 3.1 SATNN model architecture

181 *INSERT Figure 2 NEAR HERE*

182 SATNN adopts a three-stage architecture that its structure sketch is illustrated in Figure 2. In
 183 the first stage, G_s , as a generator, can produce several time series X_{ijl} with proper sampling
 184 frequencies which are interpolated from the original series X . The spline interpolation is
 185 applied once over the whole data set and the sequences X_{ijl} are obtained with different rates
 186 time-delay technology, in the other words, different interpolations are run each time to
 187 produce each X_{ijl} . In the second stage, dynamic sequences X' is obtained from the time series
 188 X_{ijl} . And the procedure is governed by series $\{c_{t1}, c_{t2}, \dots, c_{tq}\}$ as a result of controller C.

189 Here we can call the series $\{c_{t1}, c_{t2}, \dots, c_{tq}\}$ controlling signal, because each variable
 190 provides information about how to extract the proper parts from series X_{ijl} . In the third stage,
 191 ATNN is used for prediction based on the newly obtained sequences.

192 3.2 Algorithm

193 In the first stage, given the time series $\{X | x_i, i = 1, 2, \dots, n\}$, the three-stage architecture is
 194 summarized in Figure2. In this stage, G_s is a spline interpolation generator with parameter q
 195 equal to time window of delayed input series of ATNN in the third stage, which is equivalent
 196 to the number of neural network input nodes. q is obtained by the method named Maximum
 197 Entropy Method 1 (MEM1)(Jaynes, 1957). MEM1, that is widely used to decompose period
 198 characteristic of representative hydrologic series(Letie, 1995; Singh, 1997; Wang and Zhu,
 199 2002), is employed to estimate period of nonlinear time series. Given this period the neural
 200 network input nodes can be determined.

201 $\{SI_1, SI_2, \dots, SI_q\}$ is spline interpolation digital filter (Unser, 1999). Among them, SI_1 is
 202 a simple linear function generating the same data set as $\{x | x_j, j = 1, 2, \dots, n\}$ that is noted
 203 as $\{X_{ijl} | x_{ijl} = x_j; i = 1; j = 1, 2, \dots, n; l = 1\}$. These interpolation units are employed to
 204 interpolate the original series into the smoothed series
 205 $\{X_{ijl} | i = 1, 2, \dots, q; j = 1, 2, \dots, n; l = 1, 2, \dots, q; l \leq i\}$ with various sampling frequencies
 206 $\{f_1, f_2, \dots, f_q\}$ where f_1 is the sampling frequency of the original series. It is observed that
 207 these interpolation units play the roles that by inserting the smooth virtual data, the original
 208 series with frequency f_1 can change into various sequences X_{ijl} with frequency $i \times f_1$.
 209 Figure 3 describes the process of this stage.

210 INSERT Figure 3 NEAR HERE

211 In this stage, given the input data sequence X , the spline function can be denoted by $S(k)$
 212 where k is the time order of the sequence. The sequences from spline-interpolation units are
 213 obtained as follow as

$$\begin{aligned}
 & X_{1jl} = S(k_1), \quad k_1 = 1, 2, \dots, n \\
 & X_{2jl} = S(k_2), \quad k_2 = 1, 1\frac{1}{2}, 2, \dots, (n-1)\frac{1}{2}, n \\
 & \quad \vdots \\
 & X_{qjl} = S(k_q), \quad k_q = 1, 1\frac{1}{q}, 1\frac{2}{q}, \dots, 1\frac{q-1}{q}, 2, \dots, (n-1)\frac{1}{q}, (n-1)\frac{2}{q}, \dots, (n-1)\frac{q-1}{q}, n.
 \end{aligned} \tag{6}$$

215 In the second stage, for every current time point t , dynamic sequences X' are obtained by
 216 series $\{c_{t1}, c_{t2}, \dots, c_{tq}\}$ as a result of controller C . From the outputs of the interpolation
 217 units, $\{X_{ijl} \mid i = 1, 2, \dots, q; j = 1, 2, \dots, n; l = 1, 2, \dots, q; l \leq i\}$, a set of proportion data are
 218 extracted to form a new sequence $\{X'_t \mid x'_{it}; i = 0, 1, \dots, J-1\}$. A glide record is utilized in the
 219 whole course. The rule of extraction is as follows: firstly, all the data are the content of
 220 extraction; secondly, the record backward glides along the time direction; lastly, the
 221 beginning point is a certain original data x_j and the consequent data are those behind x_{j-1} .
 222 All the steps are illustrated in Figure 4. The new sequence is listed by Eq.7.

223 INSERT Figure 4 NEAR HERE

224

$$\begin{cases}
 x'_{t-0} = x_{1t1} \\
 x'_{t-1} = x_{2t1}, \quad x'_{t-2} = x_{2t2} \\
 \vdots \\
 \dots, \quad \dots, \quad x'_{t-J+1} = x_{q(t-q+1)q}
 \end{cases} \quad J = \frac{q(q+1)}{2}, \quad t \in [p+1, n], \tag{7}$$

226 where t is the current time and J the length of the sequence. Considering the training of the
 227 network in the next stage, the scale of t is defined as $t \in [p+1, n]$. When t differs, the X' is a
 228 dynamic sequence. After the first two stages, the time order in the original series will never
 229 work. Instead, we will focus on the order in X' . Figure 5 describes the dynamic combination
 230 of sequences in this stage. Then the indirect multi-step-ahead prediction based on the
 231 former two stages can be induced as follows:

$$\begin{cases}
 \hat{x}'_{t+p} = F(\hat{x}'_{t+p-1}, \hat{x}'_{t+p-2}, \dots, \hat{x}'_{t+1}, x'_t, \dots, x'_{t+p-\tau}) & \tau > p, \tau = 0, 1, \dots, J-1 \\
 \hat{x}'_{t+p} = F(\hat{x}'_{t+p-1}, \hat{x}'_{t+p-2}, \dots, \hat{x}'_{t+p-\tau}) & \tau \leq p, \tau = 0, 1, \dots, J-1
 \end{cases} \tag{8}$$

233 where the variable with a cap “^” denotes the prediction value.

234 INSERT Figure 5 NEAR HERE

235 In the third stage, the network consists of L layers with N^l neurons in the l th layer. The
 236 bipolar sigmoid function is applied as the activation function. In order to compare our model
 237 with other models proposed in literature, we choose the same bipolar sigmoid activation
 238 function $f(x) = \frac{2}{1+e^{-x}} - 1$. This bipolar sigmoid will generally yield an output that
 239 approaches 1 or -1.

240 By using the spline interpolation, the typical neuron governing equations are developed as
 241 follows:

$$242 \begin{cases} net_j^l(t) = \sum_{i=1}^{N^{l-1}} w_{ji}^l o_i^{l-1}(t - \tau_{ji}^l) \\ o_j^l(t) = \sigma^l(net_j^l(t)) \end{cases} \quad \tau_{ji}^l \in \{0, 1, \dots, \tau_{\max}\}, \quad \tau_{\max} = q - 1 \quad (9)$$

243 The output of the j th neuron in the l th layer at time t is denoted by $o_j^l(t)$. The first equation
 244 depicts the governing algorithm of original typical multilayer adaptive time-delay, in which
 245 the weight and associated delay connecting the j th neuron in the l th layer to the i th neuron
 246 in the $(l-1)$ th layer are denoted by w_{ji}^l and τ_{ji}^l , respectively. It should be noted that j varies
 247 from 1 to N^l , i varies from 1 to N^{l-1} , and τ_{ji}^l varies from 0 to τ_{\max} , which is defined
 248 subsequently as the maximum delay used to represent the desired input-output map
 249 (Yazdizadeh, 2002). Moreover, most variables mentioned above, such as i, j, l, t, τ and q , are
 250 all integers. In our model, $N^l = q$ is the number of spline interpolation units, and is equivalent
 251 to the number of derivative sequences. Clearly, the input and output that involved in the
 252 involved with above equation are depicted as

$$253 \quad y(t) = \sigma \left(\sum_{i=1}^M w_i x_i(t - \tau_i) \right), \quad \tau_i = 0, 1, \dots, J - 1. \quad (10)$$

254 Moreover, in order to avoid the problem of overfitting, we use Leave-one-out
 255 cross-validation to obtain a minimum best support value.

256 4. Case studies

257 Two case studies are used to illustrate the effectiveness of SATNN's prediction. The first one
 258 is the sunspots prediction which is a classical example of a combination of periodic and
 259 chaotic phenomena and has been served as a benchmark in the statistics literature of time
 260 series. This example is used to explore the SATNN model for general MS prediction problem.
 261 The second involves the long-term forecast of monthly discharge of a real hydropower plant.
 262 The goal is to explore the algorithm efficiency to long-term hydrologic prediction.

263 4.1. Case study I: sunspots prediction

264 Data series used in this study is from the literature (Boné and Crucianu, 2002). For
 265 convenient comparison with other methods (Boné and Crucianu, 2002), the same data sets
 266 are used for calibration and validation, i.e., the sunspots average of years 1700 through 1979
 267 is chosen to train and test model for multi-step-ahead forecasting. The training set and two
 268 testing sets are selected from this data. The training set is from years 1700 through 1920 and
 269 the test sets are from years 1921 through 1954 (Set1) and years 1955 through 1979 (Set2)
 270 (shown in Figure6).

271 *INSERT Figure 6 NEAR HERE*

272 We must pay more attention in designing a proper structure for ATNN in our model. In
 273 most prediction applications, the goal is to train the network to achieve a balance between the
 274 ability of the network to respond correctly to prediction results, and its ability to spend
 275 reasonable time to get those results. Hence, a simplified network structure with three layers is
 276 employed into our model, which can effectively perform prediction. The performance that is

277 resulted from proper neural-network architecture is mainly based on two methodologies. The
 278 first methodology is the Maximum Entropy Method 1, and the second is Statistical
 279 Methodology. Firstly, With the MEM1, we get 10 as the number of input nodes for this three
 280 layers ANN. Secondly, if the conventional methods fail to calculate the system dimension, we
 281 can minimize output error of a neural network as a function of the number of hidden neurons
 282 (Gershenfeld and Weigend, 1993). This number can estimate the system dimension(Emad et
 283 al., 1998). Then a Statistical Methodology, which uses Normalized Mean Square Error
 284 (NMSE) to calculate prediction error, is implemented to determine the number of hidden
 285 neurons. The average relationship between the number of hidden units and NMSE is shown
 286 in Figure 7. It is clear that only at the point 13 on hidden units axis, both NMSE and mean of
 287 NMSE (tested for all steps ahead) have the least values. Therefore, the number of hidden
 288 units is 13. Then the structure of STANN is 10-13-1.

289 *INSERT Figure 7 NEAR HERE*

290 Three neural networks, TDNN, ATNN and our model SATNN are implemented over the
 291 sets mentioned earlier. Moreover, we also select three models from work of Boné (Boné and
 292 Crucianu, 2002). The first is a neural network based on the error back-propagation through
 293 time algorithm (RN_BPTT). This method makes use of measures computed during gradient
 294 descent and its order of complexity is the same as for BPTT. The second is recurrent neural
 295 network based on the constructive back propagation through time (RN_CBPTT), which is
 296 heuristic, a connection is considered useful if it can have an important contribution to the
 297 computation of the gradient of the error with respect to the weights. And the last is a recurrent
 298 neural network based on the exploratory back-propagation through time (RN_ECBPTT),
 299 which is also a heuristic, a sort of breadth-first search. It explores the alternatives for the
 300 location and the delay associated with a new connection by adding that connection and
 301 performing a few iterations of the underlying learning algorithm. According to the literature,
 302 these models have an input neuron, a linear output neuron, a bias unit, and a recurrent hidden
 303 layer composed of neurons with the symmetric sigmoid as activation function. We performed
 304 20 experiments for each architecture, by randomly initializing the weights in [-0.3, 0.3]. The
 305 results of the above parameters are mostly the same as those from the referenced literature.

306 In order to compare to other models, we also employ the normalized mean squared error
 307 (NMSE) which is the ratio between the MSE and the variance of the time series. Comparison
 308 among six algorithms for Set 1 is listed in Table 1. SATNN holds the holds all best result in
 309 each steps ahead prediction. For example, $NMSE_{1\text{-step-ahead}}=0.0505$, $NMSE_{2\text{-step-ahead}}=0.1283$,
 310 $NMSE_{3\text{-step-ahead}}=0.1457$, $NMSE_{4\text{-step-ahead}}=0.1457$, $NMSE_{5\text{-step-ahead}}=0.1478$,
 311 $NMSE_{6\text{-step-ahead}}=0.150$. Furthermore, the mean of them is also the best $NMSE_{\text{mean}1-6}=0.1280$.
 312 Figure 8 displays the comparison of 6-step-ahead forecasting between TDNN, ATNN and
 313 SATNN. It is observed that SATNN provides the best prediction value. The analysis of errors
 314 in 6-step-ahead prediction is illustrated can be drown in Figure 8, in which x represents
 315 observation value, y represents prediction value, R implies the correlation coefficient, and B
 316 implies the slop of the linear fit. From the figure we can observe $R_{TDNN}=0.85571$,
 317 $R_{ATNN}=0.96294$, $R_{SATNN}=0.97594$, $B_{TDNN}=0.59544$, $B_{ATNN}=1.32698$, and $B_{SATNN}=0.69952$.
 318 These results display the capacity of our model for multi-step-ahead prediction over other
 319 models.

320
 321 *INSERT Table. 1 NEAR HERE*

322
 323 *INSERT Figure 8 NEAR HERE*

324 *INSERT Figure 9 NEAR HERE*

325 Predictions for Set 2 are displayed in Table 2 and Figure 10. In them, we observe that
326 SATNN has a similar performance to RN_ECBPTT where the errors of RN_ECBPTT at the
327 step 1、2、4 are as least as $NMSE_{1\text{-step-ahead}}=0.2507$, $NMSE_{2\text{-step-ahead}}=0.8982$ and
328 $NMSE_{4\text{-step-ahead}}=1.2537$, while at step 3、5、6, SATNN are as least as
329 $NMSE_{3\text{-step-ahead}}=1.1987$, $NMSE_{5\text{-step-ahead}}=1.3536$, $NMSE_{6\text{-step-ahead}}=1.3817$, and $NMSE_{\text{mean1-6}}=1.0988$. The above results show that SATNN provides more accurate prediction for
330 single variable multi-step-ahead forecasting than other models.
331

332 *INSERT Figure 10 NEAR HERE*

333 *INSERT Table. 2 NEAR HERE*

334

335 4.2. Case study II: long-term hydrologic prediction

336 The long-term hydrologic prediction of the Manwan Hydropower plant is implemented in
337 this case study. The Manwan Hydropower plant is located on the middle reaches of the
338 Lancang river in Yunnan Province of China and is the first completed large hydropower plant
339 in the cascading hydropower development of the Lancang river. The Lancang River is a large
340 river in Asia, which originates from the Qinghai-Tibet Plateau, penetrates Yunnan from
341 northwest to the south and passes through the Laos, Burma, Thailand, Cambodia and
342 Vietnam, and finally ingresses into the South China Sea. The river is about 4,500 km long
343 and has a drainage area of 744,000 km². The Manwan Hydropower merges on the middle
344 reaches of the Lancang River and at borders of Yunxian and Jingdong counties. The
345 catchment area at the Manwan dam site is 114,500 km², the length above Manwan is 1,579
346 km, and the mean elevation is 4,000 km. The average yearly runoff is 1,230 cubic meters per
347 second at the dam site. Rainfall provides most of the runoff and snow melt accounts for 10%.
348 Nearly 70% of the annual rainfall occurs from June to September.

349 The monthly discharge from 1953 to 2003 can be obtained wholly. Constrained by the
350 change of hydrologic conditions because of dam projects, the monthly discharge series from
351 January 1988 to December 2003 (Figure 11) are selected. The data set from January 1988 to
352 December 2002 is used for training whilst that from January to December 2003 is used for
353 validation.

354 *INSERT Figure 11 NEAR HERE*

355 Three neural networks, TDNN, ATNN and SATNN are implemented over the sets (Figure
356 11). The 12-step-ahead forecasting is considered to satisfy the engineering. The NMSE are
357 employed as the forecasting accuracy measures. Figure 12 gives comparison among them.
358 Points of interval from Jan. to Jul. are similar, while the SATNN obtains more accurate
359 values than other models in Aug., and also at point of September, and especially at the peak
360 value of each year, and at end of multi-step-ahead.

361 *INSERT Figure 12 NEAR HERE*

362 Figure 13 illustrates the relationships between observations and predictions of three layers
363 ANN model. SATNN predicts better than TDNN and ATNN with the correlation coefficient
364 of 0.9395 and slope of the best fit lines of 1.0069. Whereas TDNN (the correlation
365 coefficient and slope of the best fit lines are 0.9194 and 0.9168, respectively) and ATNN (the
366 correlation coefficient and slope of the best fit lines are 0.9225 and 0.9432, respectively)
367 predicted poorly. SATNN gives the best performance of NMSE for three test sets, which are
368 $MNSE_{\text{Set1}}=0.1357$, $MNSE_{\text{Set2}}=0.1285$, and $MNSE_{\text{Set3}}=0.1111$. These results show that
369 SATNN utilization of interpolation technology and ATNN helps it in effective tackling of the
370 drawbacks of MS. Therefore, our model (SATNN) performs much better in prediction of

371 time series in comparison to the TDNN and ATNN models (Table 3). Even if we use it to
372 solve the problem of hydrologic long-term prediction, SATNN can give the effective
373 performance.
374 *INSERT Figure 13 NEAR HERE*

375 5. Conclusion

376 Hydrological time series analysis and forecasting has been an active research area over the
377 past few decades. So the need for a long ahead process in prediction is obvious. The objective
378 of this study is to present a method for improving MS prediction model for hydrologic
379 prediction with a single variable. A three-stage indirect multi-step-ahead prediction model,
380 which combines dynamic spline interpolation into multilayer ATNN, is proposed for the long
381 term hydrologic prediction. Using spline interpolation techniques and ATNN, observations
382 samples are enlarged and simultaneously the errors accumulation and propagation caused by
383 the previous prediction are decreased.

384 The results of the case studies show that SATNN model produces the best results in most
385 situations in comparison to other models. Considering the fact that sunspots prediction is a
386 benchmark in the statistics literature of time series, the application results demonstrate that
387 SATNN model can be widely applied in other fields. For the second case study, the monthly
388 discharge prediction with the 12-step-ahead was analyzed. The SATNN also performed better
389 than other models. The two case studies show that SATNN is capable of capturing potential
390 information and relationship in the time series, and provide better predictions. The SATNN
391 should become a potential method for long-term hydrologic prediction in the future.

393 Acknowledgments

394 This research was supported by the National Natural Science Foundation of China (No.50679011), Central
395 Research Grant of Hong Kong Polytechnic University (G-U162) and Hebei Province Technology Office
396 Foundation of China (No. 072135125)

397 References

- 398 Ahmad, Z. and Zhang, J., 2002. Improving long range prediction for nonlinear process modeling through
399 combining multiple neural network. Proceeding of the 2002 IEEE International Conference on Control
400 Applications 966-971.
- 401 Arora, V.K., 2002. The use of the aridity index to assess climate change effect on annual runoff. Journal of
402 Hydrology 265,164-77.
- 403 ASCE Task Committee,2000. Artificial neural networks in hydrology-II: Hydrological applications. Journal of
404 Hydrologic Engineering, ASCE 5(2) , 124-137
- 405 Atiya, A.F., El-Shoura, S.M., Shaheen, S.I., & El-Sherif, M.S., 1999. A comparison between neural network
406 forecasting techniques-case study: river flow forecasting. IEEE Transactions on Neural Networks 10 (2),
407 402-409.
- 408 Boné, R. and Crucianu, M., 2002. An evaluation of constructive algorithms for recurrent networks on
409 multi-step-ahead prediction. ICONIP'02 Proceedings of the 9th International Conference on Neural
410 Information Processing 2 547-551.
- 411 Boné, R. and Crucianu, M., 2002. Multi-step-ahead prediction with neural networks: a review, Aproches
412 Connectionistes en Sciences Economiques et en Gestion. Boulogne sur Mer, France, pp. 97-109.
- 413 Chau, K.W., 2006. Particle swarm optimization training algorithm for ANNs in stage prediction of Shing Mun
414 River. Journal of Hydrology 329(3-4), 363-367.
- 415 Chau, K.W., Wu, C.L. and Li, Y.S., 2005. Comparison of several flood forecasting models in Yangtze River.
416 Journal of Hydrologic Engineering- ASCE 10(6), 485-491.
- 417 Cheng, C.T., Chau, K.W., Li, X.Y. and Li, G., 2004. Developing a web-based flood forecasting system for
418 reservoirs with J2EE. Hydrological Sciences Journal 49(6), 973-986.
- 419 Cheng, C.T., Zhao, M.Y., Chau, K.W. and Wu, X.Y., 2006. Using genetic algorithm and TOPSIS for Xinanjiang
420 model calibration with a single procedure. Journal of Hydrology 316(1-4),129-140.
- 421 Day, S.P. and Davenport, M.R., 1999. Continuous-time temporal back-propagation with adaptive time delays,
422 Ohio State University.

423 Emad, E.W., Prokhorov, D.V. and Wunsch, D.C., 1998. Comparative study of stock trend prediction using time
424 delay, recurrent and probabilistic neural networks and probabilistic neural networks. *IEEE Transactions*
425 *on Neural Networks* 9(6), 1456-1469.

426 Gershenfeld, N. and Weigend, A., 1993. The future of time series: learning and understanding. *Time Series*
427 *Prediction: Forecasting the Future and Understanding the Past*.

428 Haffner, P. and Waibel, A., 1992. Multi-state time delay neural net works for continuous speech recognition.
429 *Advances in Neural Information Processing Systems* 4, 135-142.

430 Irvine, K.N., & Eberhardt, A.J.,1992. Multiplicative,season ARIMA models for Lake Erie and Lake Ontario
431 water levels. *Water Resources Bulletin* 28 (2), 385-396.

432 Islam, M.N., & Sivakumar, B. ,2002. Characterization and prediction of runoff dynamics: a nonlinear dynamical
433 view. *Advances in Water Resources* 25 (2), 179-190.

434 Ismaiylov, G.K., & Fedorov, V.M. ,2001. Analysis of long-term variations in the Volga annual runoff. *Water*
435 *Resources* 28 (5), 469-477.

436 Jaynes, E.T., 1957 Information theory and statistical mechanics *Physical Review* 106, 620-630.

437 Kahaner, D., Moler, C. and Nash, S., 1988. Numerical methods and software. Prentice Hall, Upper Saddle
438 River,NJ.

439 Karunasinghe,Dulakshi S.K., Liong ,Shie-Yui, 2006. Chaotic time series prediction with a global model:
440 Artificial neural network. *Journal of Hydrology* 323(1-4), 92-105

441 Khotanzad, A., Abaye, A. and Maratukulam, D., 1994. An adaptive recurrent neural network system for
442 multi-step-ahead hourly prediction of power system loads. *IEEE International Conference on Neural*
443 *Networks and IEEE World Congress on Computational Intelligence*, 5: 3393-3397.

444 Kisi, O., 2004.River flow modeling using artificial neural networks.*Journal of Hydrologic Engineering* 9
445 (1),60-63.

446 Letie, S.M., 1995. Maximum entropy spectral analysis of the Duero Basin *International Journal of Climatology*,
447 15(4), 463-472.

448 Lin, D.T., Dayhoff, J.E. and Ligomenides, P.A., 1995. Trajectory Production with the adaptive time-delay neural
449 network. *Neural Networks* 8(3), 447-461.

450 Lin, J.Y., Cheng, C.T. and Chau, K.W., 2006.Using support vector machines for long-term discharge prediction.
451 *Hydrological Sciences Journal* 51(4), 599-612.

452 Liong, S.Y., Phoon, K.K., Pasha, M.F.K., 2005.Efficient implementation of inverse approach for forecasting
453 hydrological time series using micro GA. *Journal Of Hydroinformatics* 7 (3), 151-163

454 Luk, K.C., Ball, J.E. and Sharma, A., 2000. A study of optimal model lag and spatial inputs to artificial neural
455 network for rainfall forecasting. *Journal of Hydrology* 227(1), 56-65.

456 Maier, H., & Dandy, G.C. , 1999. Neural networks for the prediction and forecasting of water resources
457 variables: A review of modeling issues and applications. *Environmental Modelling Software* 15, 101-124.

458 Mery, H., Moeneclaey, M. and Fechtel, S., 1998. Digital communication receivers: synchronization, channel
459 estimation, and signal processing. John Wiley & Sons, NewYork.

460 Milly, P.C.D. ,1994. Climate, soil water storage, and the average annual water balance. *Water Resoures*
461 *Research* 30, 2143-2156.

462 Mimikou, M., & Rao, A.R.,1983. Regional monthly rainfall-runoff model. *Journal of Water Resources Planning*
463 *and Management* 109 (1), 75-93

464 Ng, G.W. and Cook, P.A., , , . 1998. Real-time control of systems with unknown and varying time-delays using
465 neural networks. *Engineering Applications of Artificial Intelligence* 11(3), 401-409.

466 Parasuraman, K., Elshorbagy A., 2007.Cluster-based hydrologic prediction using genetic algorithm-trained
467 neural networks.*Journal of Hydrologic Engineering* 12 (1), 52-62.

468 Parlos, A.G., Rais, O.T. and Atiya, A.F., 2000. Multi-step-ahead prediction using dynamic recurrent neural
469 networks. *Neural Networks* 13(5), 765-786.

470 Pollock, D.S.G., 1999. A handbook of time series analysis-signal processing and dynamics. Academic Press.

471 Schafer, R.W. and Rabiner, L.R., 1973. A digital signal processing approach to interpolation. *IEEE International*
472 *Conference on Neural Networks and IEEE World Congress on Computational Intelligence*, 61(6):
473 692-702.

474 Shi, D., Zhang, H.J. and Yang, L.M., 2003. Time-delay neural network for the prediction of carbonation tower's
475 temperature. *IEEE Transactions on Instrumentation and Measurement* 52(4), 1125-1128.

476 Singh, V.P., 1997. The use of entropy in hydrology and water resource. *Hydrological Processes* 11, 587-626.

477 Sivakumar, B., Berndtsson, R., & Persson, M. ,2001. Monthly runoff prediction using phase space
478 reconstruction. *Hydrological Sciences Journal* 46 (3), 377-387.

479 Smith, J.A. ,1991. Long-range streamflow forecasting using non-parametric regression. *Water Resources*
480 *Bulletin* 27 (1), 39-46.

481 Tan, Y. and Cauwenbergh, A.V., 1999. Neural-network-based d-step-ahead predictors for nonlinear systems
482 with time delay. *Engineering Applications of Artificial Intelligence* 12(1), 21-35.

483 Tarczynski, A., Kozinski, W. and Cain, G.D., 1994. Sampling rate conversion using fractional-sample delay.
484 ICASSP: 285-288.

485 Unser, M., 1999. Splines: a perfect fit for signal and image processing. IEEE Signal Processing Magazine 16(6),
486 22-38.

487 Waibel, A., Hanazawa, T., Hinton, G., Shikano, K. and Lang, K.J., 1989. Phoneme recognition using time-delay
488 neural networks. IEEE Transactions on Acoustics, Speech, Signal Processing 37(3), 328-339.

489 Wang, D. and Zhu, Y.S., 2002. Research on Cryptic Period of Hydrologic Time Series Based on MEM1 Spectral
490 Analysis. Chinese Journal of Hydrology 22(2), 19-23.

491 Williams, R. and Zipser, D., 1995. Gradient-based learning algorithms for recurrent networks and their
492 computational complexity. Backpropagation: Theory, Architecture, and Applications (LEA)

493 Wu, C.L. and Chau, K.W., 2006. A flood forecasting neural network model with genetic algorithm. International
494 Journal of Environment and Pollution 28(3-4), 261-273.

495 Yamashita, Y., 1997. Time delay neural networks for the classification of flow regimes. Computers and
496 Chemical Engineering 21, 6367-6371.

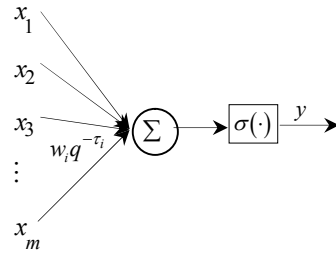
497 Yazdizadeh, A. and Khorasani, K., 2002. Adaptive time delay neural network structures for nonlinear system
498 identification. Neurocomputing 47, 207-240.

499 Yazdizadeh, A., Khorasani, K. and Patel, R.V., 2000. Identification of a two-link flexible manipulator using
500 adaptive time delay neural networks. IEEE Transactions on Systems, Man and Cybernetics, Part B,
501 30(1), 165-172.

502 Zhang, P.G., 2003. Time series forecasting using a hybrid ARIMA and neural network model. Neurocomputing,
503 50, 159-175.

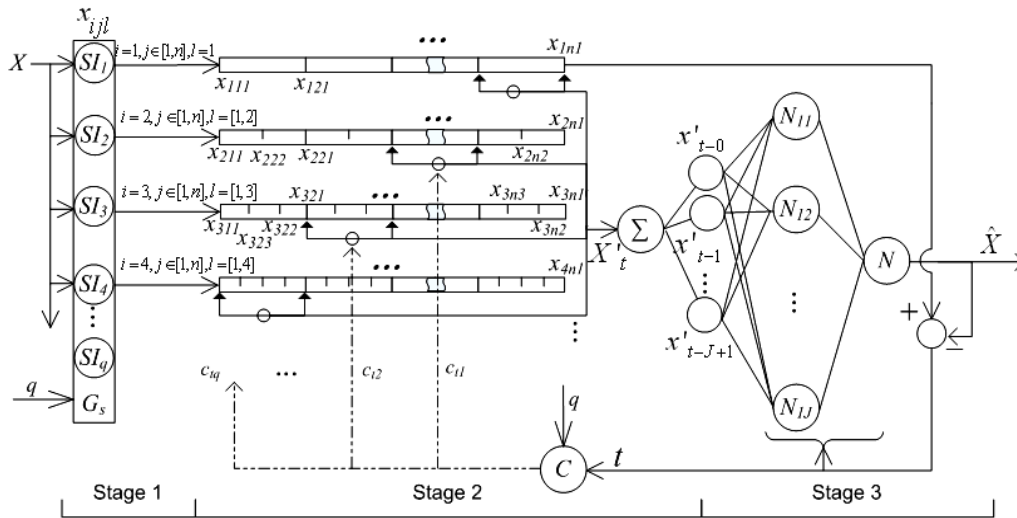
504

505



506 **Figure 1** Dynamic neuron in ATNN. $q^{-\tau}$, the shift operator. $\sigma(\cdot)$, activation function.

507



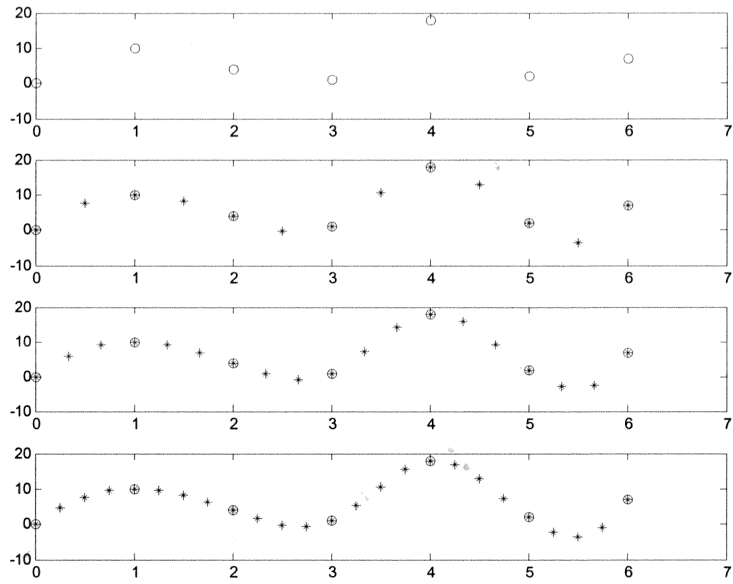
508

509

510

Figure 2 The three-stage architecture of SATNN.

511

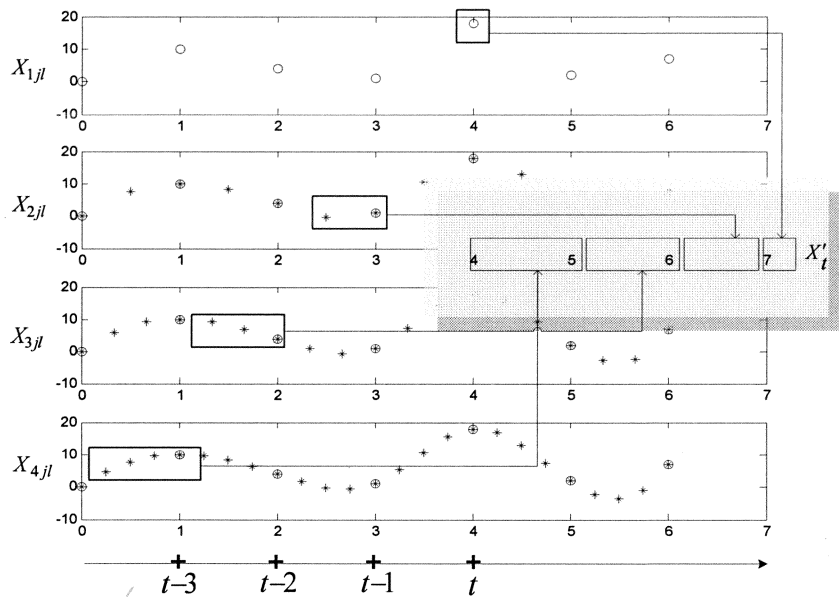


511

512

Figure 3 Sketch of sequences production by spline-interpolation units in the first stage

513

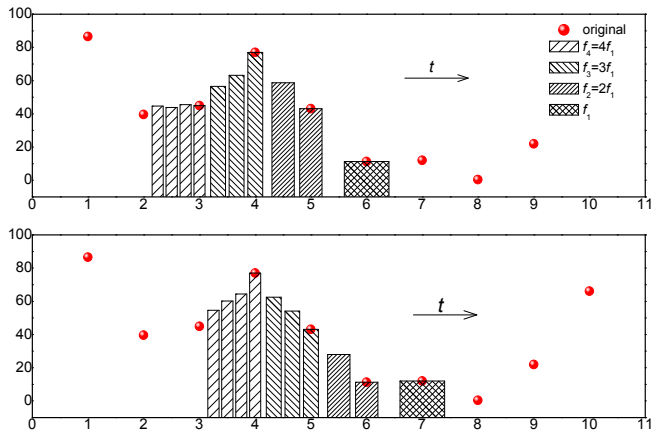


514

515

Figure 4 Dynamic sequences production in the second stage

516

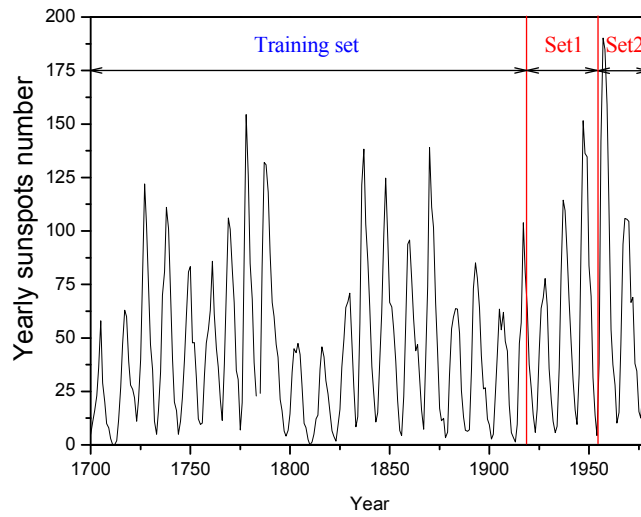


518

519

Figure 5 Dynamic sequences from the second stage

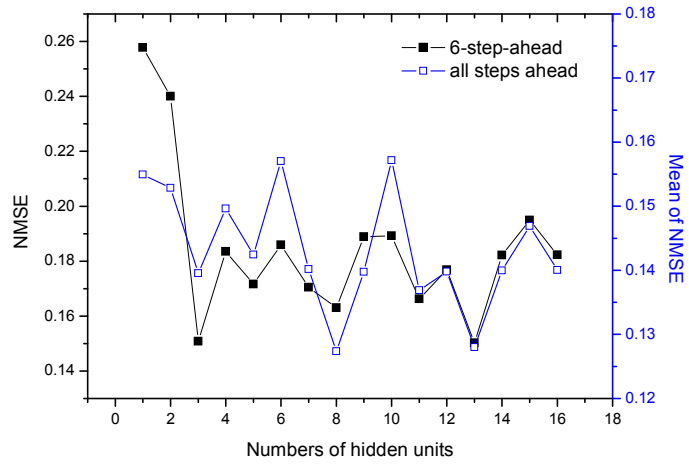
520



521

522

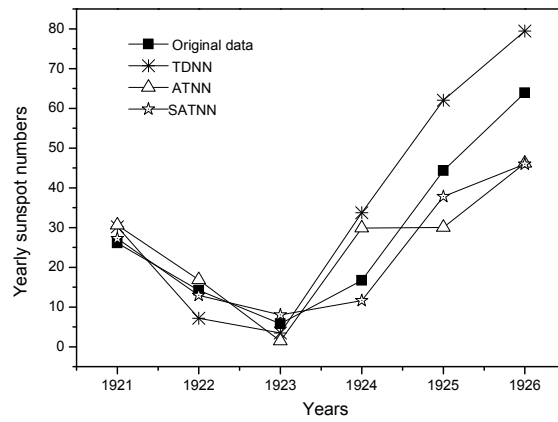
Figure 6 Training set and two test sets of yearly sunspots number



523

524 **Figure 7** Relationship between the value of hidden units and NMSE. The least NMSE can be obtained when the number of
 525 hidden units is 13.

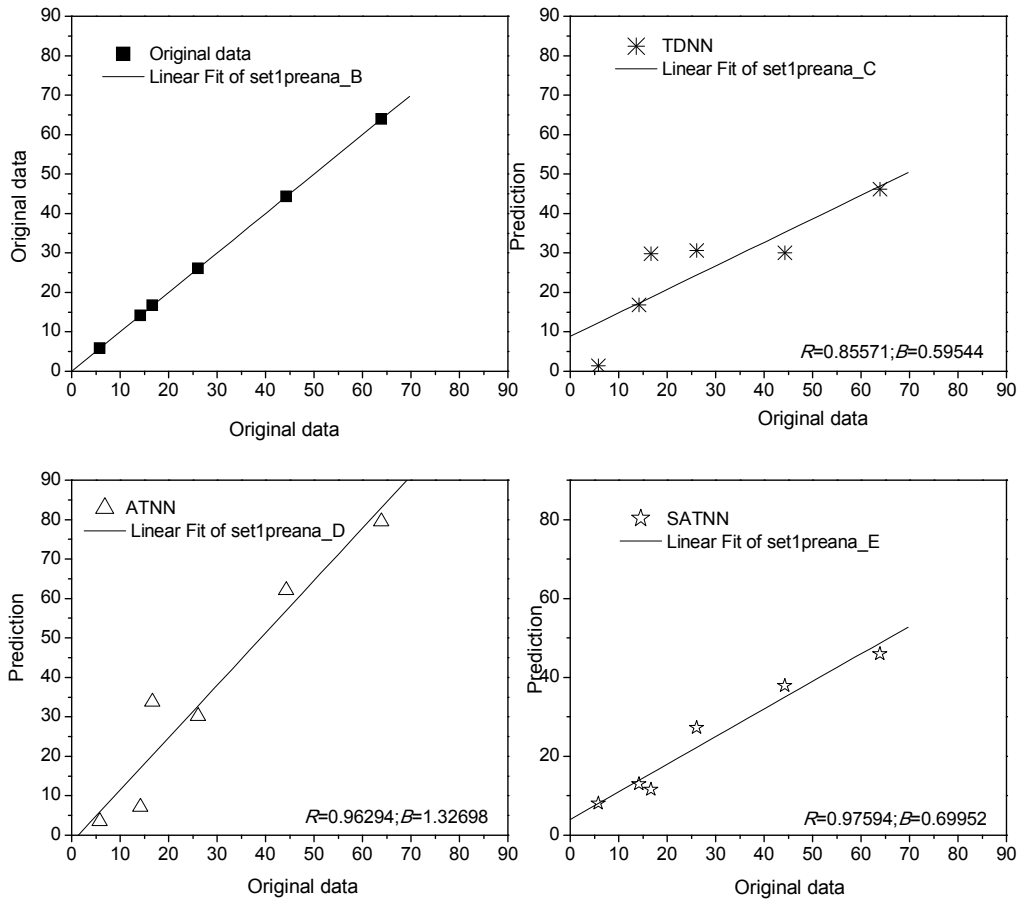
526



527

528

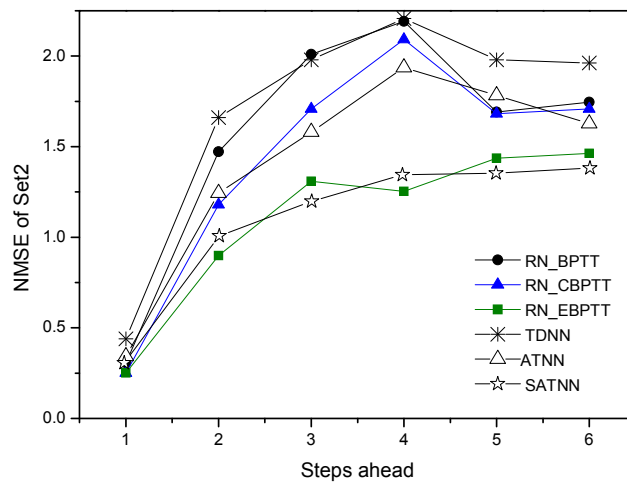
Figure 8 Best prediction results of Set1 for 6-step-ahead



529
530

531

Figure 9 Error analysis of prediction for Set1

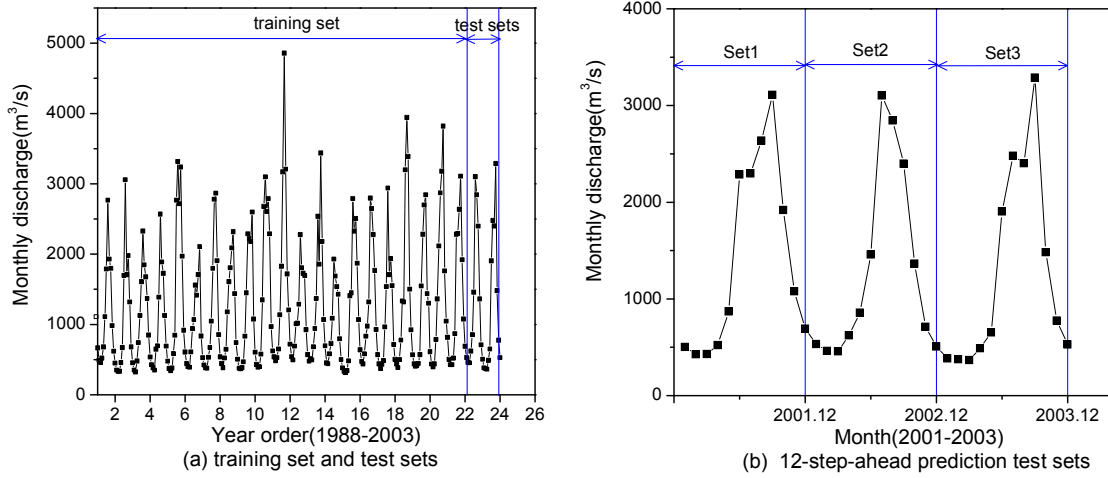


532

533

Figure 10 Prediction errors of all steps for Set2

534



535

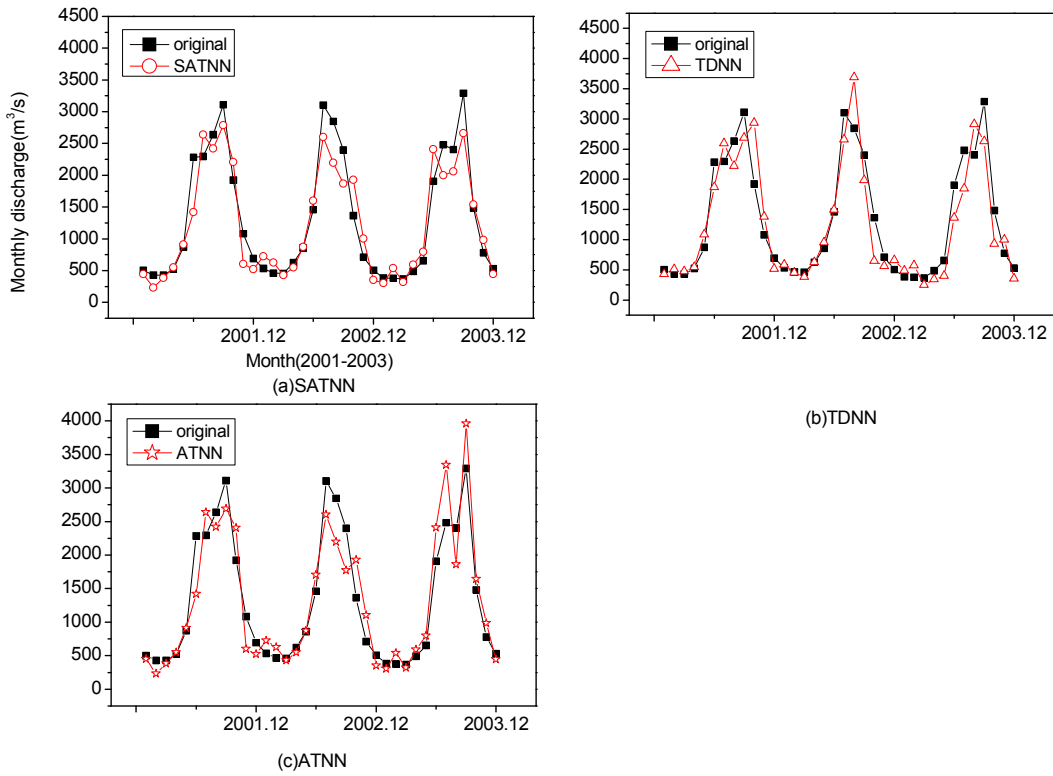
536

Figure 11 The training and test sets for 12-step-ahead prediction which are selected from the monthly runoff observation.

537

(b) is the enlarged chart of test sets in (a).

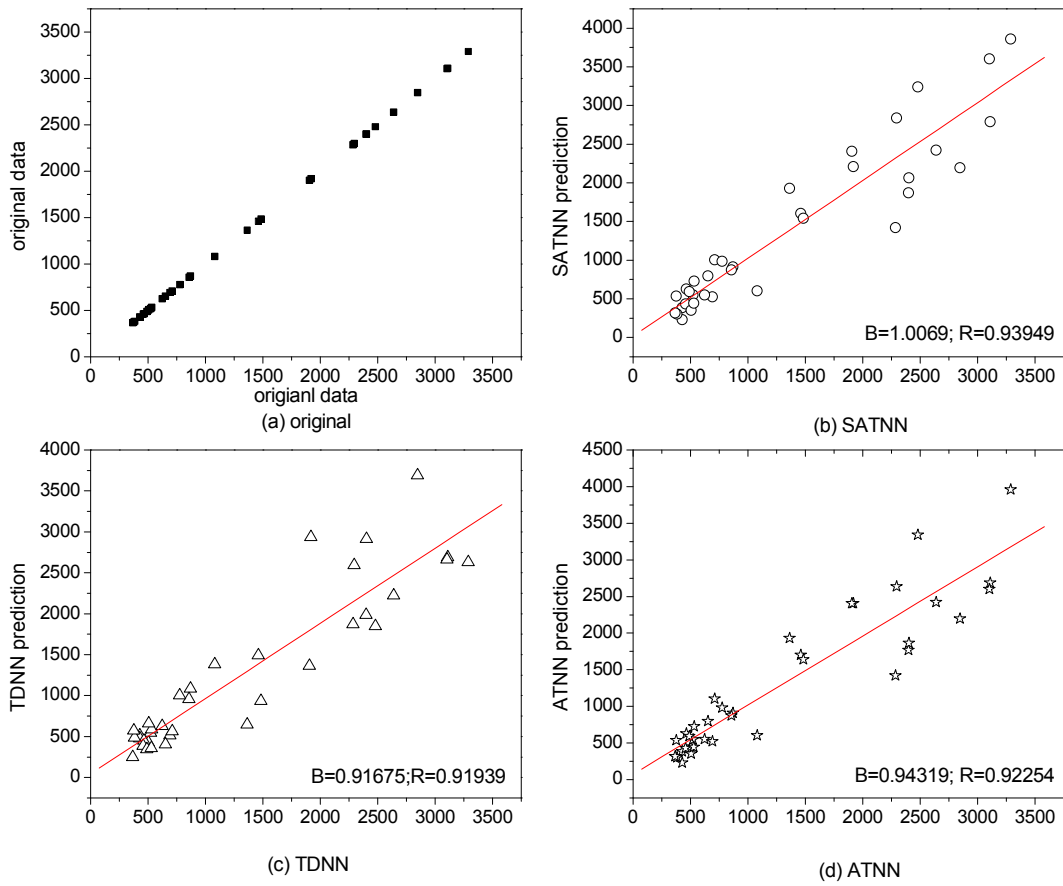
538



539

540

Figure 12 Prediction comparison among ATNN, TDNN and our model SATNN from January to December 2001~2003.



542

543 **Figure 13** Prediction error analysis of three ANN models and two main parameters of evaluation (correlation coefficient

544

and slope).

545

546

547

548

549

550

551

552

553

554

555

556

Table. 1 Comparison among six algorithms for Set1

Steps	RN BPTT [*]	RN CBPTT [*]	RN EBPTT [*]	TDNN	ATNN	SATNN
1	0.0605	0.0524	0.0519	0.0554	0.0522	0.0505
2	0.5015	0.4063	0.2677	0.4863	0.3063	0.1283
3	0.5354	0.4668	0.3805	0.5166	0.4068	0.1457
4	0.5273	0.5015	0.4322	0.5115	0.4315	0.1457
5	0.5096	0.4926	0.4491	0.5126	0.4726	0.1478
6	0.4757	0.4668	0.3628	0.5081	0.4608	0.1501

mean ₁₋₆	0.4350	0.3977	0.3240	0.4318	0.3550	0.1280
---------------------	--------	--------	--------	--------	--------	---------------

557

Note:* (Boné and Crucianu, 2002)

558

Table 2 The comparison among several predictions for Set2 with six algorithms

Steps	MNSE _{RN_BPTT}	MNSE _{RN_CBPTT}	MNSE _{RN_EBPTT}	MNSE _{TDNN}	MNSE _{ATNN}	MNSE _{SATNN}
1	0.3061	0.2507	0.2507	0.4396	0.3423	0.3061
2	1.4720	1.1807	0.8982	1.6612	1.2445	1.0077
3	2.0096	1.7087	1.3083	1.9799	1.5816	1.1987
4	2.1917	2.0915	1.2537	2.2078	1.9372	1.3448
5	1.6910	1.6814	1.4358	1.9799	1.7822	1.3536
6	1.7456	1.7087	1.4631	1.9614	1.6273	1.3817
mean ₁₋₆	1.5693	1.4369	1.1016	1.7049	1.4192	1.0988

559

560

Table 3 The comparison of prediction error analysis among three algorithms for Set1, Set 2 and Set3

	MNSE _{Set1}	MNSE _{Set2}	MNSE _{Set3}
SATNN	0.1357	0.1285	0.1111
TDNN	0.1567	0.1448	0.1534
ATNN	0.1403	0.1484	0.1499

561

562

563